Journal of Bioscience and Bioengineering
VOL. 128 No. 3, 255–263, 2019

www.elsevier.com/locate/jbiosc

Overexpression system for recombinant RNA in *Corynebacterium glutamicum* using a strong promoter derived from corynephage BFK20

Shuhei Hashiro,[1] Mayu Mitsuhashi,[1] and Hisashi Yasueda[1,2,*]

Institute for Innovation, Ajinomoto Co., Inc., 1-1 Suzuki-cho, Kawasaki-ku, Kawasaki 210-8681, Japan[1] *and Research and Development Center for Precision Medicine, University of Tsukuba, 1-2 Kasuga, Tsukuba-shi, Ibaraki 305-8550, Japan*[2]

Received 17 January 2019; accepted 7 March 2019
Available online 7 May 2019

In recent years, it has been shown that recombinant RNA molecules have a great potential in mRNA therapy and as novel agricultural pesticides. We developed a fundamental system for efficient production of target RNA molecules in *Corynebacterium glutamicum*, composed of a strong promoter named F1 and a terminator derived from corynephage BFK20 in a high-copy number plasmid vector. As a target model RNA for overexpression, we designed and used an RNA molecule [designated U1A*-RNA, ~160 nucleotides (nt) long] containing a stem/loop II (SL-II, hairpin-II) structure from U1 small nuclear RNA (snRNA), which binds to U1A protein, forming a U1 sn-ribonucleoprotein, which is essential in the pre-mRNA splicing process. *C. glutamicum* strains harboring the U1A*-RNA expression plasmid were cultured and the total RNA was analyzed. We observed prominent expression of RNA corresponding to the U1A*-RNA transcript along with lower expression of a 3′-region-truncated form of the transcript (~110 nt) in an *rnc* (encoding RNase III)-deficient strain. We also found that the produced U1A*-RNA bound to the U1A RNA-binding domain protein, which was separately prepared with *C. glutamicum*. In a batch cultivation using a fermentor, the total accumulated amount of the target RNA reached about 300 mg/L by 24 h. Thus, our results indicated that our system can serve as an efficient platform for large-scale preparation of an RNA of interest.

© 2019, The Society for Biotechnology, Japan. All rights reserved.

[**Key words:** BFK20; *Corynebacterium glutamicum*; Corynephage promoter; High gene dosage; RNA binding protein; RNA overproduction; Recombinant RNA; *rnc*]

Recently, RNAs have been demonstrated to be useful as agricultural insecticides (1–3) and as therapeutic agents (4,5). In nucleic acid-based medicine, the expectation for therapeutic oligonucleotides such as anti-oligo nucleotides and siRNA has been increasing. These drugs are produced by a chemical synthesis method because of the low degree of base polymerization in the sequence. However, in the case of mRNA therapy, an enzymatic or biological production method is required for efficient and accurate synthesis of long nucleic acid chains. RNA is also gaining attention as a novel agricultural pesticide named RNA insecticides. Its action mechanism is growth inhibition of pest insects by suppressing crucial gene expression via RNA interference (RNAi) caused by double-stranded RNA (dsRNA) against the target pest (3,6,7). Thus, especially when considering the use of RNA as an insecticide, it is indispensable to economically produce the target RNA molecule of interest at low costs and in large-scale using a biological production system.

In recombinant RNA production using microorganisms, several production systems using a combination of T7 RNA polymerase and T7 promoter in *Escherichia coli* have been reported (8–11). With the use of RNA in the pharmaceutical field in mind, Ponchon and colleagues (12,13) have developed an RNA production system that produces the target RNA precursor in *E. coli*, from which the desired RNA fragment molecule can be prepared with precise structure. As the tRNA molecule is not readily degraded *in vivo*, they incorporated the desired RNA region in the characteristic structural backbone of tRNA (designated tRNA scaffold) and succeeded in stably expressing the precursor RNA *in vivo*. Using a similar method, it has also been reported that target RNA can be produced using part of the 5S rRNA as a stable structural scaffold to improve the *in vivo* stability of the target RNA (14). In addition, a unique method for producing target RNA using RNA-dependent RNA polymerase of bacteriophage Phi6 infecting *Pseudomonas* has been reported (15). However, it seems that these production methods are not sufficiently productive and stable to cope with industrial mass production of the recombinant RNA of interest.

Here, to produce a defined RNA molecule with a target nucleotide sequence we propose an alternative host: the gram-positive microorganism, *Corynebacterium glutamicum*, which is a safe and traditional production strain of L-glutamate approved as Generally Recognized As Safe (GRAS). *C. glutamicum* has been industrially used for decades to produce huge amounts of several amino acids (16–18), and it exhibits robustness even in large-scale production and in many fermentation processes. These fundamental characteristics are especially suitable for the mass production of useful materials like RNA insecticides by fermentation. An indispensable prerequisite for establishing an RNA production system is the use of a strong promoter for efficient transcription. For this purpose, we

---

[*] Corresponding author at: Institute for Innovation, Ajinomoto Co., Inc., 1-1 Suzuki-cho, Kawasaki-ku, Kawasaki 210-8681, Japan. Tel.: +81 44 245 8554; Fax: +81 44 244 9617.

E-mail address: hisashi_yasueda@ajinomoto.com (H. Yasueda).

1389-1723/$ – see front matter © 2019, The Society for Biotechnology, Japan. All rights reserved.
https://doi.org/10.1016/j.jbiosc.2019.03.003

decided to use a promoter derived from bacteriophages infecting *Corynebacterium*. Corynephage BFK20 is a lytic bacteriophage isolated from the industrial amino acid producer, *Brevibacterium* (*Corynebacterium*) *flavum* CCM 251 (19), and the genome sequence has been completely determined (20). Koptides et al. (19) have found a DNA fragment with strong promoter activity within both *E. coli* and *C. glutamicum*, and named it F1 promoter. In their study, the strong F1 promoter and a bi-directional transcription terminator (Ter) were identified in the phage genome, however, detailed studies on the F1 promoter and the terminator have not been performed yet.

For a vector carrying the expression system of target RNAs, it is typically desirable to use a stable plasmid with a high-copy number. Thus, we tried to increase the gene-dosage of the RNA-expression unit by high-copy number plasmids derived from pVC7N (21), which is a shuttle vector between *E. coli* and *C. glutamicum*. In a previous study, we isolated the high-copy number vectors, pVC7H1 and pVC7H2, of which the copy number in *C. glutamicum* was more than 100 and 300 per chromosome, respectively (21). RNA metabolism is determined by the balance between the biosynthesis and degradation; various RNases are involved in the degradation of RNA. Among them, ribonuclease III (RNase III) is an endoribonuclease specific for dsRNA. In particular, suppression of RNase III activity seems to be a critical point in the production of dsRNA molecules and RNA species forming complex secondary structures. In *E. coli*, RNase III, encoded by the *rnc* gene, plays multiple roles in the processing of rRNA and mRNA, but it is not essential for survival (22). Recently, Maeda et al. (23) have constructed an *rnc* mutant in the *C. glutamicum* R strain by disrupting the *cgR_1959* gene. They reported that RNase III is also not essential for survival of this strain. In *C. glutamicum* strain ATCC 13869 (also named strain 2256, DDBJ/EMBL/GenBank accession no. AP017557), the locus tag of *CGBL_0119780* is also annotated as *rnc* gene (24).

As a model target RNA for overexpression in this study, we selected an RNA sequence containing part of U1 small nuclear RNA (U1 snRNA), which is a component of the spliceosomal U1 small nuclear ribonucleoprotein particles (U1 snRNP) involved in pre-mRNA splicing (25,26). U1A protein is a component of the U1 snRNP and binds specifically to U1 snRNA via the stem/loop II (SL-II, hairpin-II) region composed of about 40 nucleotides (nt). Hall and Stump (26) have demonstrated the specific binding between the first 102 amino acid residues of U1A protein and a short RNA substrate from the SL-II structure. Thus, we used a target RNA (designated U1A*-RNA) designed to have a characteristic structure (the SL-II region) that binds to the RNA-binding domain (designated U1A-RBD) of U1A protein as the counterpart (Fig. 1).

As mentioned above, efficient and mass production of recombinant RNAs for various applications is highly desired, thus we conducted this study. Here, we report the overexpression of U1A*-RNA as a model of recombinant RNA produced by *C. glutamicum* as a host cell. Construction of an RNA expression system with a strong promoter in a high-copy number vector in a *C. glutamicum* RNase III-deficient strain, achieved a remarkable production of the objective RNA molecule.

MATERIALS AND METHODS

Strains, plasmids, DNA primers and media The bacterial strains and plasmids used in this study are listed in Table 1. *C. glutamicum* 2256LΔ*rnc* is a derivative of strain 2256L (21), and was used as the main host strain for RNA production. Strain YPS010 [formally named YDK010:phoS(W302C)] (27) was used for protein production. *C. glutamicum* strains were routinely grown on CM-Dex medium (28) at 30°C. YPS010 was cultured as described previously (27). *E. coli* JM109 was used as a host for construction of recombinant plasmids and was cultured in Luria–Bertani (LB) medium at 37°C. When appropriate, antibiotics were added as follows: chloramphenicol (Cm) at 5 mg/L and 25 mg/L for *C. glutamicum* and *E. coli*, respectively; kanamycin (Km) at 25 mg/L for both strains. All DNA primers used in this study are listed in Table S1 and were obtained from Eurofins Genomics (Tokyo, Japan).

Plasmid construction The RNA expression plasmids, pVC-U1A*-1, pVH1-U1A*-1 and pVH2-U1A*-1, were generated as follows. DNA fragment-A (0.4 kbp) composed of the F1 promoter from BFK20 (20) and a DNA segment encoding the target RNA (U1A*-RNA) including the Ter sequence of BFK20 (20) was chemically synthesized and prepared (Eurofins Genomics) (Fig. 2). Using fragment-A as a template, DNA-fragment-B containing the U1A*-RNA expression unit was prepared by PCR amplification with primers P01 and P02. A vector DNA fragment-C derived from pVC7N (21) was obtained by PCR with primers P03 and P04. Then,

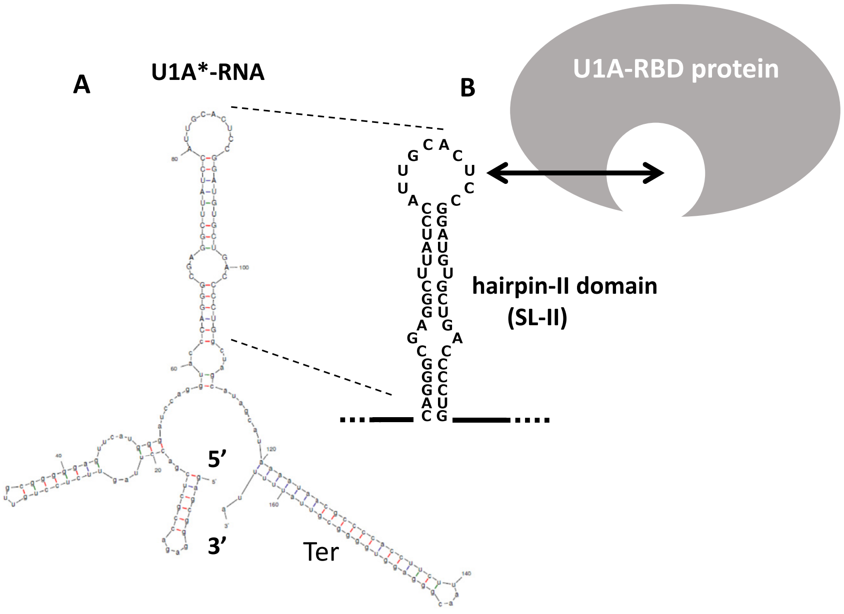

FIG. 1. Structure of U1A*-RNA as a target RNA and its interaction with U1A-RBD protein. (A) Predicted secondary structure of U1A*-RNA. Ter indicates terminator region derived from BFK20. (B) Schematic diagram showing the specific binding between U1A*-RNA and U1A-RBD protein through the hairpin-II (SL-II) domain of the target RNA.

TABLE 1. Bacterial strains and plasmids used in this study.

Strain or plasmid	Relevant characteristic(s)[a]	Reference
Strain		
Corynebacterium glutamicum		
2256	ATCC 13869, AJ1151, wild-type strain	24
2256L	2256 derivative cured a cryptic plasmid pAM330N	21
2256LΔrnc	*rnc* mutant of 2256L	This study
YDK010	Mutant of 2256 by *N*-methyl-*N*′-nitro-*N*-nitrosoguanidine, Δ*cspB*	27
YPS010	*phoS* (W302C) of YDK010	27
Escherichia coli		
JM109	*endA1*, *recA1*, *gyrA96*, *thi*, *hsdR17* (r_K^-, m_K^+), *relA1*, *supE44*, λ^-, Δ*(lac-proAB)*, F′[*traD36*, *proAB*$^+$, *lacI*^{q}, *lacZ*ΔM15]	Takara-Bio
Plasmid		
pAM330N	Cryptic plasmid in *C. glutamicum* 2256	21
pVC7N	*C. glutamicum–E. coli* shuttle vector derived from pAM330N and pHSG329; Cm^r	21
pVC7H1	pVC7N *copA1* mutant; Cm^r	21
pVC7H2	pVC7N *copA2* mutant; Cm^r	21
pVC-U1A*-1	pVC7N derivative carrying U1A*-RNA expression unit; Cm^r	This study
pVH1-U1A*-1	pVC7H1 derivative carrying U1A*-RNA expression unit; Cm^r	This study
pVH2-U1A*-1	pVC7H2 derivative carrying U1A*-RNA expression unit; Cm^r	This study
pPK4	*Corynebacterium–E. coli* shuttle vector, pHM1519-ori, pUC-*ori*; Km^r	27
pPK6	pPK4 derivative carrying *tatABC* from *C. glutamicum*; Km^r	27
pPK-tU1A-2	pPK6 derivative for expression of U1A-RBD protein; Km^r	This study
pRACE	A vector for In-Fusion cloning; pUC-*ori*; Ap^r	Takara Bio
p5′RACE-U1A	pRACE derivative carrying 5′RACE-PCR fragment of U1A*-RNA; Ap^r	This study
p3′RACE-U1A	pRACE derivative carrying 3′RACE-PCR fragment of U1A*-RNA; Ap^r	This study
p5′RACE-U1AS	pRACE derivative carrying 5′RACE-PCR fragment of U1A*S-RNA; Ap^r	This study
p3′RACE-U1AS	pRACE derivative carrying 3′RACE-PCR fragment of U1A*S-RNA; Ap^r	This study
pBS4S	pHSG299 derivative containing *sacB* gene from *Bacillus subtilis*, Km^r	31
pBS4SΔrnc	pBS4S derivative ^{a}arrying a truncated *rnc* (*Δrnc*) gene; Km^r	This study

[a] Cm^r, resistance to chloramphenicol; Km^r, resistance to kanamycin; Ap^r, resistance to ampicillin.

fragment-B was ligated with fragment C for the construction of pVC-U1A*-1, using an In-Fusion HD Cloning Kit (Takara Bio, Shiga, Japan). For the construction of pVH1-U1A*-1 and pVH2-U1A*-1, high-copy number vectors pVC7H1 and pVC7H2 were used (21), respectively, instead of pVC7N.

U1A-RBD protein was produced as a fusion protein with pro-protein glutaminase (pro-PG) from *Chryseobacterium proteolyticum* (29) using the Tat secretory system of *C. glutamicum* (30). The expression plasmid, pPK-tU1A-2 (Fig. S3) was constructed as follows. For the expression unit of the fused U1A-RBD protein, DNA fragment-D comprising the promoter sequence of *C. glutamicum cspB*, the coding sequences of the *E. coli* TorA signal peptide, the pro-PG protein, a linker peptide and U1A-RBD fused with a His (×6)-tag, was prepared based on chemical synthesis and *in vivo* cloning. The DNA segment-E of the expression unit was amplified by PCR using primers P05 and P06, and fragment-D as the template. A vector fragment-F was prepared by PCR using primers P07 and P08, and pPK6 (27) as the template. Then, both DNA fragments E and F were ligated using an In-Fusion HD Cloning Kit to construct pPK-tU1A-2.

Plasmid pBS4SΔ*rnc* for deleting *rnc* in *C. glutamicum* 2256L was constructed using the integration vector, pBS4S (31). Genomic DNA was extracted and purified from *C. glutamicum* 2256L with a DNeasy Blood & Tissue kit (Qiagen, Tokyo, Japan). Using DNA as a template, a 1.0-kbp fragment of the 5′-flanking sequence of *rnc* was amplified using primers P09 and P10, and another 1.0-kbp fragment of the 3′-flanking sequence was obtained by PCR using primers P11 and P12. A vector DNA fragment of pBS4S was amplified by PCR using primers P13 and P14, and was ligated with both *rnc*-flanking fragments by an In-Fusion HD kit to construct pBS4SΔ*rnc*. The polymerase for the PCR reactions used in this study was PrimeSTAR GXL DNA polymerase (Takara Bio).

Construction of the *rnc* gene deletion mutant of *C. glutamicum* Strain 2256L was transformed with pBS4SΔ*rnc* by electroporation and obtained transformants were then grown at 30°C for 24 h on CM-Dex agar medium containing kanamycin. After incubation of some transformants at 30°C for 24 h in CM-Dex medium without kanamycin, the cultures were plated on Dex-S10 agar medium (28) and grown at 30°C for 24 h. Sucrose-resistant and kanamycin-sensitive colonies in which the plasmid DNA was lost from the chromosome were selected. After *rnc* deletion mutants were confirmed by PCR amplification of the *rnc* locus in the genome, an *rnc* deletion mutant was selected from the candidates and was designated strain *C. glutamicum* 2256LΔ*rnc*.

Production of recombinant RNA and its PAGE analysis For small-scale culture, transformants were cultured in 2 mL of CM-Dex medium containing chloramphenicol in test tubes at 30°C for 18 h with shaking at 120 rpm. Total RNA was prepared from 200 μL of culture. The culture was mixed with 400 μL of RNAprotect Bacteria reagent (Qiagen), and centrifuged at 5000 ×g for 10 min to recover the bacterial cells. After the cell pellet was resuspended in 225 μL of Tris/EDTA buffer containing 15 mg/mL lysozyme and incubated at 25°C for 30 min,

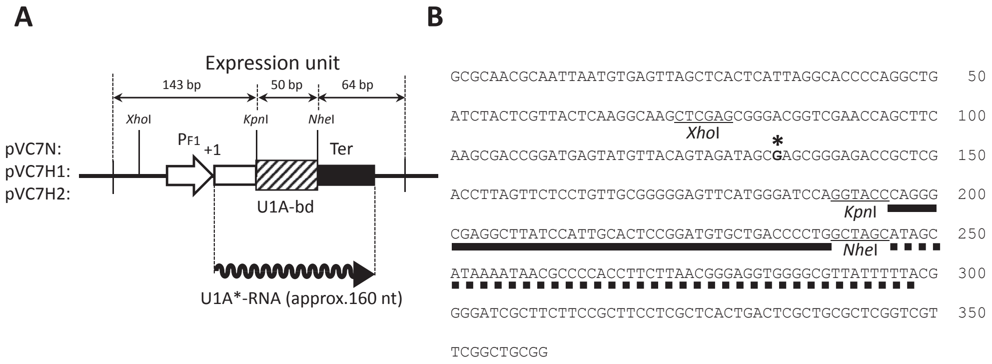

FIG. 2. U1A*-RNA expression unit. (A) Schematic diagram of the expression unit of U1A*-RNA. F1 promoter (P_{F1}) and transcription terminator (Ter) are indicated with an open arrow and a black thick bar. The U1A-bd segment indicated with hatched lines shows the region including the hairpin-II domain in U1 snRNA. pVC7N, pVC7H1 and pVC7H2 were used as vectors of the expression unit. The wavy line with an arrowhead represents the transcript of U1A*-RNA of about 160 nt. (B) DNA fragment composed of F1 promoter and the coding region of U1A*-RNA including the Ter sequence. An asterisk shows the transcription start site from P_{F1}. Bold and dashed lines indicate the hairpin-II region and Ter region, respectively. Representative restriction sites (XhoI, KpnI and NheI) are also indicated.

25 μL of 20 mg/mL proteinase K (Takara Bio) were added, followed by incubation at 25°C for another 30 min. Then, the suspension was mixed with 750 μL of TRIzol LS (Thermo Fisher Scientific, Tokyo, Japan) and RNA was isolated according to the manufacturer's protocol. Finally, the sample was resolved with 50 μL of RNase-free water and loaded on non-denaturing PAGE (Novex, TBE-gel, 6%, Thermo Fisher). RNA samples were electrophoresed and stained with SYBR Green II (Takara Bio). For batch fermentation using a fermentor, transformants were inoculated in 300 mL of modified MMTG medium (named RPB1 medium) in which $CaCl_2$ was removed (27) and the concentration of glucose and KH_2PO_4 was increased to 120 g/L and 3.5 g/L, respectively. The fermentation was performed at 30°C, pH 7.0, with 1/1 vvm (volume of air per volume of medium per minute) of aeration and agitating to ensure P_L (oxygen partial pressure of liquid phase) of at least 5%. An aliquot of the cultures was appropriately diluted for measuring cell density at 620 nm (OD_{620}). RNA quantification was carried out as follows. DynaMarker RNA Low II (BioDynamics Lab, Tokyo, Japan), as a standard marker for RNA quantification, was electrophoresed on a PAGE gel in parallel with the RNA sample of interest. After staining the gel with SYBR Green II, the fluorescence of RNA was detected with the gel imaging analyzer, ChemiDoc XRS (Bio-Rad, Tokyo, Japan), and the amount of target RNA was quantified by the image analysis software Quantity One (Bio-Rad).

Preparation of U1A-RBD protein and N-terminal amino acid sequence analysis A fused U1A-RBD protein for electrophoretic mobility shift assay (EMSA) was produced by *C. glutamicum* YPS010 harboring pPK-tU1A-2. The transformant was cultured in MMTG medium at 30°C for 58 h (27). The supernatant of the culture was separated from the cells by centrifugation (13,800 ×g, 2 min) and filtrated with Mini-UniPrep (0.45 μm, GE Healthcare, Tokyo, Japan). Then, the His (×6)-tagged U1A-RBD protein was purified from the sample using Capturem His-Tagged Purification Kit (Takara Bio). After the concentration and the buffer-exchange of the eluate by Amicon Ultra centrifugal filters (30 kDa), the fraction containing the fused U1A-RBD protein was prepared for EMSA. The protein concentration was determined using the Pierce BCA Protein Assay Kit (Thermo Fisher), and the purity was analyzed by SDS-PAGE as follows. The protein sample was mixed with NuPAGE LDS Sample Buffer and NuPAGE reducing agent, and heated at 70°C for 10 min. Then, it was applied onto a NuPAGE 4–12% Bis-Tris Protein Gel, and proteins were stained with SimplyBlue SafeStain (Thermo Fisher).

For N-terminal amino acid sequencing, the fused U1A-RBD protein sample (8 μg in total) was electrophoresed on NuPAGE gel and blotted onto a polyvinylidene difluoride membrane (0.2 μm pore size) using the iBlot 2 Dry system (Thermo Fisher). After staining with SimplyBlue SafeStain, the protein band of interest was cut out and subjected to Edman degradation in a PPSQ-33A sequencer (Shimadzu, Kyoto, Japan).

5′ and 3′ RACE Total RNA extracted from the cells was loaded on a PAGE gel as described above. Two target RNA bands, U1A*-RNA and another band (named U1A*S-RNA in Fig. 3), were excised from the stained gel. After chopping each gel piece containing the target RNA, RNA was eluted by incubation in TBE buffer (100 mM Tris, 90 mM boric acid, 1 mM EDTA) at 37°C for 3 h. The supernatant was recovered and precipitated with isopropanol to prepare each target RNA sample. Then, to identify both the 5′ and 3′ ends of the RNA transcripts, 5′ and 3′ RACE PCR analyses were carried out. Each RNA sample (2 μg) was poly(A) tailed using a Poly(A) tailing kit (Thermo Fisher). After TRIzol LS extraction, the RNA with a poly(A) tail was purified by ethanol precipitation. The first strand cDNA was synthesized using a SMARTer RACE 5′/3′ kit (Takara Bio). The cDNA fragments corresponding to the 5′ and 3′ RACE PCR fragments of each sample were amplified with a combination of Universal primer A (supplied with the kit) and gene-specific primers P15 and P16, respectively (Table S1). The resulting PCR products were cloned into the pRACE vector included in the In-Fusion cloning kit to generate p5′RACE-U1A, p3′RACE-U1A, p5′RACE-U1AS and p3′RACE-U1AS. The inserted DNA fragments of five to twelve plasmid clones were individually sequenced using primers P17 and P18.

Electrophoretic mobility shift assay (EMSA) U1A*-RNA was prepared as described above. The RNA was labeled using an RNA 3′-End Biotinylation kit (Thermo Fisher), according to the manufacturer's manual. Approximately 0.5 ng, 5 ng, and 50 ng of each purified U1A-RBD protein was incubated for 30 min at 25°C with the labeled U1A*-RNA (0.85 ng) in 20 μL of binding buffer [10 mM HEPES, pH 7.3, 20 mM KCl, 1 mM $MgCl_2$, 1 mM DTT, 5% (v/v) glycerol, 0.1 μg/μL of tRNA] using a LightShift Chemiluminescent RNA EMSA Kit (Thermo Fisher). As a competition inhibitor, a synthetic RNA fragment (18-nt) (32) of the SL-II sequence (5′-GGGCAUUGCACUCCGCCC-3′), obtained from Eurofins Genomics, was used. For competition experiments, the specific competitor was added to the reaction solution containing 50 ng of the protein before the labeled probe RNA was added to the mixture. The resulting binding solutions were mixed with the loading buffer and loaded onto a 6% PAGE, and then RNA and protein complexes were detected according to the manufacturer's instructions (Thermo Fisher).

Estimation of plasmid copy number Plasmid copy number was determined using quantitative PCR (qPCR) as described previously (21). As targets for qPCR analysis, two genes, *repA* in the objective pAM330N-replicon-containing plasmid and *dnaA* on the *C. glutamicum* chromosome, were selected and the plasmid copy number was calculated as the ratio of quantified *repA* to *dnaA* using samples from three independent experiments. Standard curves displaying the cycle threshold parameter (Ct) values plotted against the log of the initial DNA concentration were generated using pGEM-RD2 (21), which was designed to contain both *dnaA* and *repA* target regions for qPCR amplification.

RNA secondary structure analysis The RNA secondary structure was predicted using the mfold web server (http://unafold.rna.albany.edu/?q=mfold/RNA-Folding-Form) (33) and the CentroidFold program (http://www.ncrna.org/centroidfold) (34).

RESULTS

Construction of a recombinant RNA overexpression system For the genetic construction of a recombinant RNA overexpression system, we first selected the F1 promoter and Ter-sequence derived from corynephage BFK20 (20) for high-level transcription and strong termination, respectively. Although the details of the promoter have not been characterized, it has been indicated that the F1 promoter works strongly in *C. glutamicum* (19). Thus, the DNA sequences of the 143 nt containing the F1 promoter region and of the 64 nt including Ter were used in the construction of the RNA production unit (Fig. 2). A target RNA named U1A*-RNA was designed to be composed of about 160 nt including a U1A protein-binding domain (SL-II domain) (Fig. 1). A possible secondary structure of the U1A*-RNA transcript was predicted by the mfold software (33) (Fig. 1A), and a similar secondary structure of the recombinant RNA was predicted by the CentroidFold software (34) (Fig. S1).

The RNA expression unit was initially cloned into the pVC7N vector to construct pVC-U1A*-1. As the copy number of pVC7N was estimated to be about 10–20 copies per chromosome in *C. glutamicum* (21), we further generated another two kinds of RNA-expression plasmids based on the high-copy number mutant vectors, pVC7H1 and pVC7H2 (21) to increase the gene dosage of the RNA expression unit in the host cell, *C. glutamicum*. The resultant plasmids were named pVH1-U1A*-1 and pVH2-U1A*-1, respectively (Fig. 2A).

Production of U1A*-RNA in *C. glutamicum* Each of the constructed expression plasmids for U1A*-RNA was introduced into *C. glutamicum* 2256L, to generate the corresponding transformants. After these strains were cultured, total RNA was extracted from each culture to examine the expression of the target RNA. However, no significant RNA band corresponding to U1A*-RNA was detected in the non-denaturing PAGE analysis (Fig. 3A). Thus, it seemed that the target RNA produced by this system was promptly degraded by RNases in the host strain. As it was inferred that the target RNA molecule retains many double-stranded regions by complicated secondary structures (Fig. 1A), we subsequently investigated the expression of the target RNA in the RNaseIII-deficient strain (*C. glutamicum* 2256LΔ*rnc*). A distinct RNA band with a presumed size of about 160 nt was clearly confirmed by PAGE in each of the three samples (Fig. 3A). In particular, the expression level of the presumed U1A*-RNA produced by pVH2-U1A*-1 was surprisingly very high, judging by the abundance ratio relative to the inherent 5S rRNA and tRNAs of the host cells. As expected, the amount of target RNA positively correlated with the copy number of the vector plasmids used. This result also indicated that the *rnc* gene defect in *C. glutamicum* was quite effective for the *in vivo* production of the possible U1A*-RNA.

In addition, along with the prominent RNA band of interest, a slightly smaller RNA band of about 110 nt was observed (Fig. 3A). As the abundance ratio of these two bands was similar in the three samples, we thought that the smaller RNA transcript was derived from or associated with the main RNA transcript, not from RNA of the host cells. Thus, structural analysis of these two RNA transcripts was performed as described in the next section.

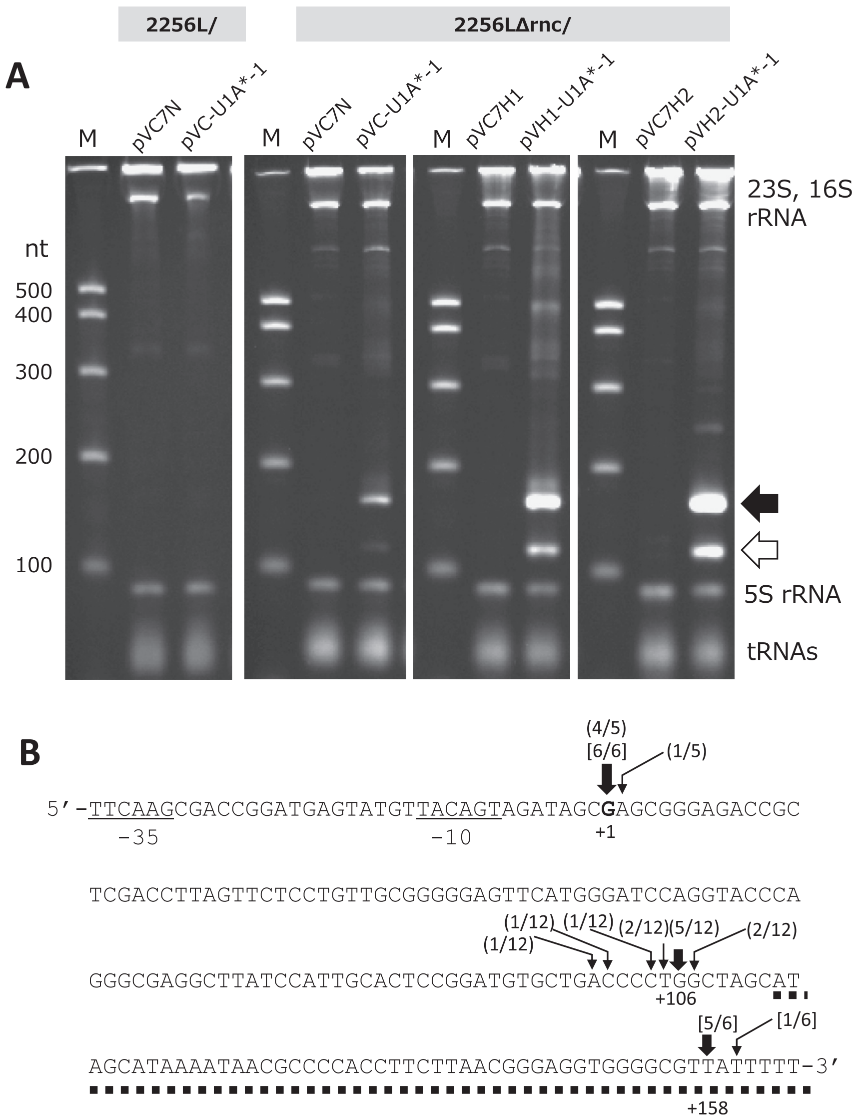

FIG. 3. Productivity and structural analysis of U1A*-RNA produced by *C. glutamicum*. (A) PAGE analysis of RNAs produced in *C. glutamicum*. Lane M is a size marker of single-stranded RNAs. Samples from the 2256L strain harboring pVC7N as a negative control and pVC-U1A*-1, as well as from 2256LΔ*rnc* harboring pVC7N, pVC7H1, pVC7H2, pVC-U1A*-1, pVH1-U1A*-1 or pVH2-U1A*-1, were electrophoresed on 6% PAGE. A prominent RNA band corresponding to U1A*-RNA and its truncated forms (U1A*S-RNA) are indicated by a black arrow and an open arrow, respectively. Endogenous RNA species (23S, 16S rRNAs, 5S rRNA and tRNAs) from the host cells are also shown. (B) Determination of the 5′ and 3′ ends of the produced U1A*-RNAs (U1A*-RNA and its truncated forms) by RACE analysis. Both 5′ and 3′ terminals of the transcripts are indicated by arrows, and the analysis results of U1A*-RNA and U1A*-RNA are shown in square brackets and parentheses, respectively. The fraction in the brackets represents the number of clones in which a transcript started or terminated at that position per number of clones examined. The F1 promoter is underlined and the Ter sequence is indicated with dashed lines. The transcription starting point is assigned as +1 and the positions of the 3′ end of the two major transcripts (bold arrows) are indicated with the nucleotide number below the DNA sequence.

Structural characterization of the overexpressed RNAs To structurally evaluate the produced RNAs, we determined both the 5′ and 3′ ends of the products using the 5′ and 3′ RACE technique. Analysis of the main RNA molecule mapped the 5′ end to nucleotide G corresponding to the transcription start site of the F1 promoter (Figs. 3B and S2) in all six independent sequences obtained by 5′ RACE. Analysis of the 3′ RACE fragments derived from the main RNA placed the 3′ end closely to two uridines (U) of the Ter structure (in sequences of six clones analyzed; Fig. 3B). Thus, we concluded that the RNA produced by this system was U1A*-RNA, as expected. Similarly, both ends of the smaller RNA transcript (~110 nt) were analyzed in five clones for the 5′ end and in 12 clones for the 3′ end. The 5′ end was dominantly mapped to the same G residue at a rate of 4/5, and the other one was mapped to the adjacent nucleotide A as the 5′ end nucleotide of the transcript. However, the 3′ ends of 12 clones were mapped to nucleotides in front of the Ter structure (Figs. 3B and S2). This result implied that the smaller RNA corresponds to a 3′-truncated form of U1A*-RNA, thus we named it U1A*S-RNA. Finally, the transcript length of U1A*-RNA and its truncated form was of 158–160 and 99–107 nucleotides, respectively; these sizes are mostly consistent with the approximate sizes estimated from the PAGE analysis.

Preparation of fused U1A-RBD protein for binding assay Functional activity of the produced U1A*-RNA was examined by the interaction between U1A*-RNA and U1A-RBD protein by EMSA. U1A-RBD protein was designed to be expressed and secreted by fusing it with pro-PG via a flexible peptide linker, using the *C. glutamicum* secretion system (Figs. S3 and S4), because pro-PG can be efficiently secreted with the TorA twin arginine signal peptide by the Tat secretion system and expressed in an adequate conformation ready to form an active PG structure (36). Additionally, the fused U1A-RBD protein was designed with a His (×6)-tag at its C-terminus to facilitate its purification. After the expression plasmid for the fused U1A-RBD protein was constructed and introduced into *C. glutamicum* YPS010, the expression of the fused U1A-RBD was investigated in the culture medium. A dominant protein band with a size corresponding to the presumed U1A-RBD fusion protein (49.1 kDa) was observed on the SDS-PAGE analysis of the culture medium (Fig. S5). When the culture supernatant was loaded onto a His-trap Ni-column and eluted with imidazole, the protein of interest was selectively purified, indicating that the protein had a His-tag at the C-terminal region (Fig. S5, lane 2). Subsequently, the N-terminal amino acid sequence of the purified protein was determined. We identified the sequence, Asp-Ser-Asn-Gly-Asn, which are the first five amino acids of pro-PG. Analyses of the N-terminal amino acid sequence and the molecular weight indicated that the protein secreted by this system was the fused U1A-RBD protein in which the TorA signal sequence for secretion was correctly removed. In this way, the protein containing U1A-RBD was prepared for EMSA of U1A*-RNA.

Specific binding of U1A*-RNA and U1A-RBD protein To examine the binding activity of U1A*-RNA, EMSA using the fused U1A-RBD protein was performed. The EMSA results demonstrated that U1A*-RNA bound to U1A-RBD *in vitro* (Fig. 4), even though the affinity was not very strong. As a competitive inhibitor of the binding, an RNA fragment with a sequence forming the SL-II structure known to bind U1A protein (26) was prepared. We found that the U1A*-RNA binding clearly decreased by the addition of excess synthetic RNA fragment, indicating that the binding of U1A*-RNA to U1A-RBD was specific.

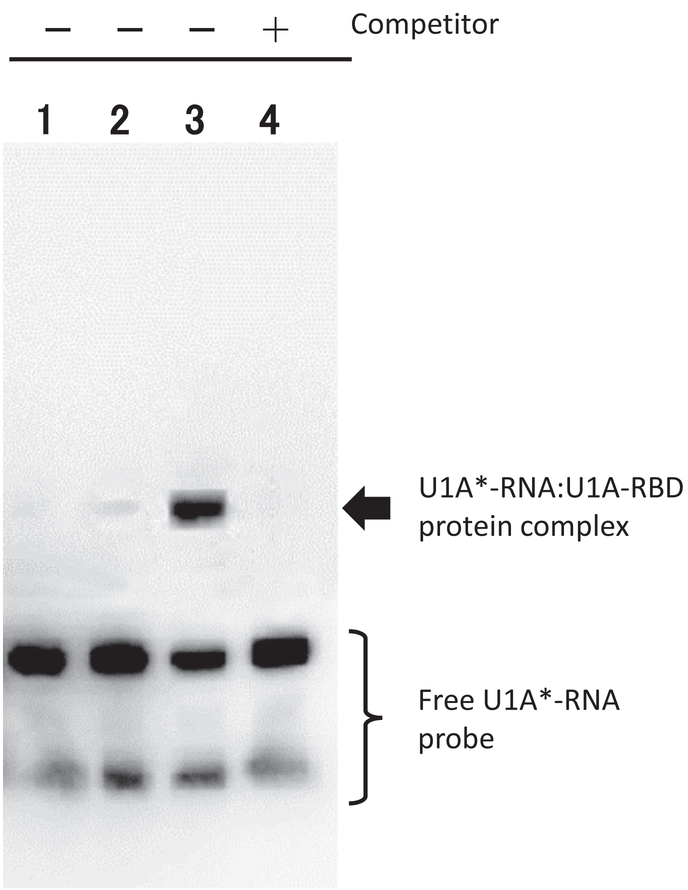

FIG. 4. EMSA of U1A*-RNA binding to U1A-RBD protein. EMSA analysis of U1A*-RNA, performed with increasing concentrations (lanes 1 to 3) of the fused U1A-RBD protein by a factor of 10 from 11 nM, and with addition of a 200-fold molar excess of a competitor (lane 4).

Overexpression of U1A*-RNA in *C. glutamicum* In the test tube cultivation, *C. glutamicum* 2256LΔ*rnc* harboring pVH2-U1A*-1 displayed the highest expression of the target RNAs including U1A*S-RNA. Next, we cultured the RNA-producing strain and a control strain in a fermentor capable of supplying higher oxygen at a high cell density to increase the production of the target RNAs. Unexpectedly, both strains presented similar growth curves (Fig. 5A), indicating that the U1A*-RNA expression in the strain was not a major burden on growth and metabolism. Furthermore, the accumulation of the target RNAs including the truncated form reached the maximum after 24 h of fermentation, and the target RNA accumulation amount was estimated to be about 300 mg/L (Fig. 5 and Table 2). In addition, the accumulation of the target RNAs gradually decreased with the duration of the culturing process. This suggests that degradation of the target RNAs still occurred by some RNase other than RNase III, or by an intracellular condition. Evaluation of the copy number of the two plasmids, pVC7H2 and pVH2-U1A*-1, in this batch fermentation revealed that the copy numbers in the *C. glutamicum* 2256LΔ*rnc* strain were 272 ± 5.1 and 332 ± 17.1, respectively, at 21 h after starting the culture. These values are similar to the copy number of the pVC7H2 vector in *C. glutamicum* 2256L strain (20).

DISCUSSION

In this study we constructed a fundamental system for the efficient production of recombinant RNA using *C. glutamicum* as a host strain. To identify a strong promoter suitable for the mass production of target RNA, we first carried out preliminary transcriptome analysis by RNAseq of *C. glutamicum* 2256L that was transformed with a plasmid carrying a DNA fragment from the BFK20 genome. The analysis indicated that a large amount of transcript was transcribed from the F1 promoter, and suggested that the transcriptional activity of the F1 promoter was strong (Hashiro, S. and Yasueda, H., unpublished data). The strength of transcription was directly compared with that of two representative promoters used for protein expression in *C. glutamicum*, derived from *cspB* encoding the major cell surface protein PS2, and *gapA* encoding glyceraldehyde 3-phosphate dehydrogenase (30,35–37). Each promoter was linked to the coding region of the target RNA and their expression levels were examined in *C. glutamicum* 2256LΔ*rnc* (Fig. S6). In present culture conditions, the expression of recombinant RNA under the control of both promoters was much lower than under the F1 promoter (Fig. S7). Based on these results, we chose to use the F1 promoter of corynephage for high expression of recombinant RNA. Majtan et al. (38) have shown that the F1 promoter is situated in a group of genes expressed at the early stage of phage development, but implied that it could be expressed at the beginning of the late stage. However, based on the U1A*-RNA expression from this promoter over time in the cultivation of *C. glutamicum*, we concluded that the F1 promoter was highly activated in the logarithmic growth phase of *C. glutamicum* (Fig. 5). Thus, we presumed that the F1 promoter was recognized by RNA polymerase with σ^A factor in *C. glutamicum*. The −10 region (5′-TACAGT-3′) and the −35 region (5′-TTCAAG-3′) of the F1 promoter have been presumed to be the promoter elements (38), but our analysis of the 5′ end of the U1A*-RNA transcript identified the start point of the transcript from the F1 promoter (Fig. 3B). The −10 sequence has a high similarity to the consensus recognition sequence (5′-gnTAnanTng-3′) (39) of σ^A-RNA polymerase in *C. glutamicum*, but the −35 sequence did not show apparent homology with the consensus sequence.

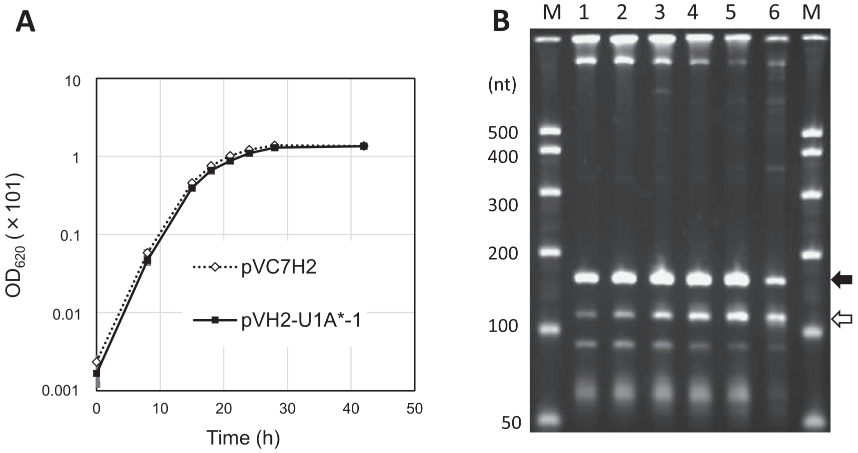

FIG. 5. Production of U1A*-RNA in *C. glutamicum* 2256LΔ*rnc* harboring pVH2-U1A*-1 in batch fermentation. (A) Growth of *C. glutamicum* 2256LΔ*rnc* harboring pVCH2 as a control or pVH2-U1A*-1. Average values and standard deviations of three independent experiments are shown. (B) PAGE analysis of total RNA prepared from *C. glutamicum* 2256LΔ*rnc* harboring pVH2-U1A*-1 during fermentation. Lanes: M, ssRNA marker; 1, 15 h; 2, 18 h; 3, 21 h; 4, 24 h; 5, 28 h; 6, 42 h of culture. Closed and open arrows indicate the positions of U1A*-RNA and U1A*S-RNA, respectively. Shown is a representative performance in the RNA production experiment by a jar fermentor.

TABLE 2. Accumulation amount of total U1A*-RNA during a batch-fermentation of *C. glutamicum*[a] 2256LΔ*rnc* harboring pVH2-U1A*-1.

Culture time (h)	Total U1A*-RNA (mg/L)[a]
15	183.1 ± 9.2
18	219.8 ± 4.1
21	258.3 ± 13.2
24	307.9 ± 3.9
28	308.0 ± 7.9
42	111.4 ± 6.8

[a] Mean values ± standard deviation of three independent experiments are shown.

In the expression system using the F1 promoter, special substance or culturing conditions for transcriptional induction are unnecessary. In the *E. coli* RNA expression systems, several studies (8–11) used the T7 promoter expression system for target RNA expression, in which the production of T7 RNA polymerase must be induced by an inducer such as isopropyl β-D-thio-galactoside (IPTG) at a relatively early growth phase of the host *E. coli* strain. In this process, it will be rather difficult to obtain a large amount of bacterial cell mass producing the target RNA, therefore it is disadvantageous for the objective of mass production of target RNA at a low cost.

As a transcriptional terminator for this expression system, we used the Ter sequence derived from the same corynephage genome (20). A transcript of the Ter region can potentially form a long hairpin structure with an inverted repeat of 20 nt. Therefore, as expected, in the main fraction of produced U1A*-RNAs, the 3′ ends were located in the U residues following the GC-rich region of the Ter segment (Figs. 3B and S2). In addition, partial generation of truncated forms of the transcript was confirmed. The 3′ ends of the truncated species were mapped extensively in the stem portion of SL-II. From the predicted secondary structure of U1A*-RNA, a relatively AU-rich single-stranded region appeared to be located between SL-II and the strong SL structure formed by Ter (Fig. S2). Therefore, generation of the truncated form may be the result of cleavage of the single-stranded region as a target by endogenous endonuclease and gradual decomposition of the target RNA strand from the cleaved end by a 3′-to-5′ exonuclease. One candidate for the endonuclease is RNase E/G in *C. glutamicum*, which is known to cleave *aceA* mRNA encoding isocitrate lyase in a single-stranded region between the two SL structures formed in its 3′-UTR (40). A model was proposed in which the exonuclease degrades *aceA* mRNA from the truncated end to the upstream region. Therefore, to suppress the generation of such truncated RNA, it is considered necessary to first delete RNase E/G that may trigger this decomposition. Additionally, if the nucleotide sequence of the single-stranded region does not greatly affect the function of the target RNA molecule, a solution such as altering part of the sequence to be decomposed should be considered.

The copy number of this RNA expression unit was amplified using a high-copy mutant plasmid vector (21) with the aim of increasing the target RNA expression. Indeed, at 21 h of this RNA production, the copy number of the expression plasmid was estimated to be about 300. In *C. glutamicum*, there are only six *rrn* genes in the genome (24), but rRNA is still dominant in the total RNA present in the growing cell. This is speculated to be the reason that most of the rRNAs are associated with ribosomal proteins, and thereby rRNAs are less likely to be attacked by endogenous RNases. Within the *C. glutamicum* cell, U1A*-RNA does not have any proteins to specifically bind to, but by co-expressing a binding protein (such as U1A-RBD) as an intracellular protein in cells expressing U1A*-RNA, this target RNA may be more stabilized by protection from RNase attack, resulting in improved accumulation of the target RNA in the cells.

In the U1A*-RNA expression system, a characteristic RNA structure could potentially be formed in which three SL structures are created before and after the SL-II region (Fig. 1A). That is, the first small SL structure and the second SL structure can be formed immediately downstream of the 5′ end of the transcript and a strong SL structure derived from the Ter sequence is generated on the 3′ terminus. Thus, we speculated that the characteristic structure may block to some extent prompt attacks by any exoribonucleases from both ends, and thus U1A*-RNA can highly accumulate. In addition, as we considered that the produced U1A*-RNA forms such a complicated conformation with many double-stranded regions *in vivo*, it was speculated that the *rnc* gene deficiency greatly contributed to the accumulation of the target RNA (Fig. 3A). Ponchon and Dardel (13) have used the tRNA scaffold as a structural backbone for expressing arbitrary RNAs, based on the fact that the tRNA structure is highly resistant to RNA degradation *in vivo*. In addition, Liu et al. (14) have used part of the 5S rRNA structure for protection from RNA degradation. Therefore, similar to these strategies, it can be inferred that the structure of this expression system can also be used as a new kind of scaffold backbone for efficient expression of target recombinant RNA.

In this study, the functionality of the U1A*-RNA produced was investigated by specific binding to U1A-RBD protein (Fig. 4). For the preparation of the fused U1A-RBD protein, we designed a fusion protein with pro-PG and prepared it by expression through the Tat secretory system (30). Proteins secreted by the Tat system are secreted after the formation of the folded conformation inside the cell (41). Pro-PG is a representative protein secreted as a soluble enzyme suitable for exerting enzyme activity by the Tat system in *C. glutamicum* (30). Therefore, because the fused U1A-RBD protein was produced with the functionally structured pro-PG, we deduced that U1A-RBD also retained the original conformation capable of binding to the counterpart RNA molecule. Thereby, we demonstrated the functional activity of U1A*-RNA produced in this system.

The RNA content in bacteria was investigated in *E. coli*; it has been reported that rRNAs are about 80% of the total, tRNAs are about 10% and the remaining ~10% are various mRNAs and small RNAs (42). If *C. glutamicum* has the same compositional ratio of RNAs, then the accumulation level of U1A*-RNA in *C. glutamicum* should be considerably high as the produced target RNA amount was apparently larger than the content of 5S rRNA, judging by the PAGE analysis (Figs. 3A and 5B). In the production of recombinant RNA using *E. coli* as a host, the examples of chimeric RNA expression with tRNA-scaffold revealed the production yields to be around several milligrams to 50 mg per liter of culture medium (13). In the RNA expression system with 5S rRNA as the scaffold, no obvious numerical value for the amount of target RNA production was reported, but it was estimated to be similar to that of the maximum endogenous 5S rRNA content (14). Using the *P. syringae* strain expression system, the amount of recombinant RNA was reported to be 1.6 mg dsRNA/g wet cells in a fermentor (15), but details of the productivity remain unspecified. On the other hands, in our simple batch fermentation for RNA production, accumulation of about 300 mg/L was achieved. The target RNA expression level in this research seems to be the highest yield reported for a recombinant RNA, so far. In the jar fermentation test, the growth of the RNA-producing strain presented a growth pattern almost similar to that of the control strain, indicating that the RNA accumulation in this strain was not burdensome to the host cell. Therefore, this suggests that there is room for further productivity improvement of target RNA production using *C. glutamicum* as a host strain. Furthermore, taking advantage of the high fermentation stability and robustness at the industrial level of *C. glutamicum* as a microbial workhorse, we will be able to improve the productivity of target RNAs with specific purposes. In particular, we will study the production method of long-chain RNAs that can be applied in the fields of nucleic acid medicine and dsRNA necessary for agriculture based on this fundamental production system.

Supplementary data to this article can be found online at https://doi.org/10.1016/j.jbiosc.2019.03.003.

ACKNOWLEDGMENTS

We are grateful to A. Ando (WDB-Eureka), Y. Shimono (WBD) and Y. Iseki (Persol Tempstaff Co.) for their technical assistance. We express our gratitude to Dr S. Umekage (Toyohashi University of Technology) for his technical advice on RNA manipulation. We also wish to thank Drs Y. Matsuda and M. Date (Ajinomoto Co.) for valuable comments on the experiment of recombinant protein production and protein analysis, respectively. We thank Edanz Group for editing the English text of a draft of this manuscript.

References

1. **Zotti, M., dos Santos, E. A., Cagliari, D., Christiaens, O., Taning, C. N. T., and Smagghe, G.:** RNA interference technology in crop protection against arthropod pests, pathogens and nematodes, Pest Manag. Sci., **74**, 1239–1250 (2018).
2. **Palli, S. R.:** RNA interference in Colorado potato beetle: steps toward development of dsRNA as a commercial insecticide, Curr. Opin. Insect Sci., **6**, 1–8 (2014).
3. **Christiaens, O., Prentice, K., Pertry, I., Ghislain, M., Bailey, A., Niblett, C., Gheysen, G., and Smagghe, G.:** RNA interference: a promising biopesticide strategy against the African sweetpotato weevil *Cylas brunneus*, Sci. Rep., **6**, 38836 (2016).
4. **Steinle, H., Behring, A., Schlensak, C., Wendel, H. P., and Avci-Adali, M.:** Concise review: application of in vitro transcribed messenger RNA for cellular engineering and reprogramming: progress and challenges, Stem Cell., **35**, 68–79 (2017).
5. **Davidson, B. L. and McCray, P. B., Jr.:** Current prospects for RNA interference-based therapies, Nat. Rev. Genet., **12**, 329–340 (2011).
6. **Bolognesi, R., Ramaseshadri, P., Anderson, J., Bachman, P., Clinton, W., Flannagan, R., Ilagan, O., Lawrence, C., Levine, S., Moar, W., and other 6 authors:** Characterizing the mechanism of action of double-stranded RNA activity against Western corn rootworm (*Diabrotica virgifera virgifera* LeConte), PLoS One, **7**, e47534 (2012).
7. **Choi, M.-Y., Vander Meer, R. K., Coy, M., and Scharf, M. E.:** Phenotypic impacts of PBAN RNA interference in an ant, *Solenopsis invicta*, and a moth, *Helicoverpa zea*, J. Insect Physiol., **58**, 1159–1165 (2012).
8. **Tenllado, F., Martínez-García, B., Vargas, M., and Díaz-Ruíz, J. R.:** Crude extracts of bacterially expressed dsRNA can be used to protect plants against virus infections, BMC Biotechnol., **3**, 3 (2003).
9. **Nelissen, F. H. T., Leunissen, E. H. P., van de Laar, L., Tessari, M., Heus, H. A., and Wijmenga, S. S.:** Fast production of homogeneous recombinant RNA–towards large-scale production of RNA, Nucleic Acids Res., **40**, e102 (2012).
10. **Yin, G., Sun, Z., Liu, N., Zhang, L., Song, Y., Zhu, C., and Wen, F.:** Production of double-stranded RNA for interference with TMV infection utilizing a bacterial prokaryotic expression system, Appl. Microbiol. Biotechnol., **84**, 323–333 (2009).
11. **Kaur, G., Cheung, H.-C., Xu, W., Wong, J. V., Chan, F. F., Li, Y., McReynolds, L., and Huang, L.:** Milligram scale production of potent recombinant small interfering RNAs in *Escherichia coli*, Biotechnol. Bioeng., **115**, 2280–2291 (2018).
12. **Ponchon, L., Beauvais, G., Nonin-Lecomte, S., and Dardel, F.:** A genetic protocol for the expression and purification of recombinant RNA in *Escherichia coli* using a tRNA scaffold, Nat. Protoc., **4**, 947–959 (2009).
13. **Ponchon, L. and Dardel, F.:** Large scale expression and purification of recombinant RNA in *Escherichia coli*, Methods, **54**, 267–273 (2011).
14. **Liu, Y., Stepanov, V. G., Strych, U., Wilson, R. C., Jackson, G. W., and Fox, G. E.:** DNAzyme-mediated recovery of small recombinant RNAs from a 5S rRNA-derived chimera expressed in *Escherichia coli*, BMC Biotechnol., **10**, 85–93 (2010).
15. **Aalto, A. P., Sarin, L. P., van Dijk, A. A., Saarma, M., Poranen, M. M., Arumäe, U., and Bamford, D. H.:** Large-scale production of dsRNA and siRNA pools for RNA interference utilizing bacteriophage Φ6 RNA-dependent RNA polymerase, RNA, **13**, 422–429 (2007).
16. **Yasueda, H.:** Overproduction of L-glutamate in *Corynebacterium glutamicum*, pp. 165–176, in: Anazawa, H. and Shimizu, S. (Eds.), Microbial production. Springer, Tokyo (2014).
17. **Kimura, E.:** L-Glutamate production, pp. 439–463, in: Eggeling, L. and Bott, M. (Eds.), Handbook of *Corynebacterium glutamicum*. Taylor & Francis, Boca Raton, FL (2005).
18. **Ikeda, M. and Takeno, S.:** Amino acid production by *Corynebacterium glutamicum*, pp. 107–147, in: Yukawa, H. and Inui, M. (Eds.), *Corynebacterium glutamicum*, biology and biotechnology. Springer-Verlag, Berlin, Heidelberg (2013).
19. **Koptides, M., Barák, I., Šišová, M., Baloghová, E., Ugorčaková, J., and Timko, J.:** Characterization of bacteriophage BFK20 from *Brevibacterium flavum*, J. Gen. Microbiol., **138**, 1387–1391 (1992).
20. **Bukovska, G., Klucar, L., Vlcek, C., Adamovic, J., Turna, J., and Timko, J.:** Complete nucleotide sequence and genome analysis of bacteriophage BFK20-A lytic phage of the industrial producer *Brevibacterium flavum*, Virology, **348**, 57–71 (2006).
21. **Hashiro, S., Mitsuhashi, M., and Yasueda, H.:** High copy number mutants derived from *Corynebacterium glutamicum* cryptic plasmid pAM330 and copy number control, J. Biosci. Bioeng., **127**, 529–538 (2019).
22. **Court, D. L., Gan, J., Liang, Y.-H., Shaw, G. X., Tropea, J. E., Costantino, N., Waugh, D. S., and Ji, X.:** RNase III: genetics and function; structure and mechanism, Annu. Rev. Genet., **47**, 405–431 (2013).
23. **Maeda, T., Tanaka, Y., Takemoto, N., Hamamoto, N., and Inui, M.:** RNase III mediated cleavage of the coding region of *mraZ* mRNA is required for efficient cell division in *Corynebacterium glutamicum*, Mol. Biol., **99**, 1149–1166 (2016).
24. **Nishio, Y., Koseki, C., Tonouchi, N., Matsui, K., Sugimoto, S., and Usuda, Y.:** Analysis of strain-specific genes in glutamic acid-producing *Corynebacterium glutamicum* ssp. *lactofermentum* AJ1511, J. Gen. Appl. Microbiol., **63**, 157–164 (2017).

25. **Aaron, D., Krummel, P., Nagai, K., and Oubridge, C.:** Structure of spliceosomal ribonucleoproteins, F1000 Biol. Rep., **2**, 39 (2010).
26. **Hall, K. B. and Stump, W. T.:** Interaction of N-terminal domain of U1A protein with an RNA stem/loop, Nucleic Acids Res., **20**, 4283–4290 (1992).
27. **Matsuda, Y., Ito, Y., Kashima, Y., Yamada, N., Tsuru, N., and Itaya, H.:** Method for secretory production of protein, US Patent, US 2018/0037918 A1 (2018).
28. **Chinen, A., Kozlov, Y. I., Hara, Y., Izui, H., and Yasueda, H.:** Innovative metabolic pathway design for efficient L-glutamate production by suppressing CO_2 emission, J. Biosci. Bioeng., **103**, 262–269 (2007).
29. **Yamaguchi, S., Jeenes, D. J., and Archer, D. B.:** Protein-glutaminase from *Chryseobacterium proteolyticum*, an enzyme that deamidates glutaminyl residues in proteins. Purification, characterization and gene cloning, Eur. J. Biochem., **268**, 1410–1421 (2001).
30. **Kikuchi, Y., Itaya, H., Date, M., Matsui, K., and Wu, L.-F.:** TatABC overexpression improves *Corynebacterium glutamicum* Tat-dependent protein secretion, Appl. Environ. Microbiol., **75**, 603–607 (2009).
31. **Nakamura, J., Hirano, S., Ito, H., and Wachi, M.:** Mutations of the *Corynebacterium glutamicum* NCgl1221 gene, encoding a mechanosensitive channel homolog, induce L-glutamic acid production, Appl. Environ. Microbiol., **73**, 4491–4498 (2007).
32. **Endoh, T., Sisido, M., and Ohtsuki, T.:** Cellular siRNA delivery mediated by a cell-permeant RNA-binding protein and photoinduced RNA interference, Bioconjug. Chem., **19**, 1017–1024 (2008).
33. **Zuker, M.:** Mfold web server for nucleic acid folding and hybridization prediction, Nucleic Acids Res., **31**, 3406–3415 (2003).
34. **Sato, K., Hamada, M., Asai, K., and Mituyama, T.:** CENTROIDFOLD: a web server for RNA secondary structure prediction, Nucleic Acids Res., **37**, W277–W280 (2009).
35. **Lee, J.-Y., Na, Y.-A., Kim, E.-S., Lee, H.-S., and Kim, P.:** The actinobacterium *Corynebacterium glutamicum*, an industrial workhorse, J. Microbiol. Biotechnol., **26**, 807–822 (2016).
36. **Salim, K., Haedens, V., Content, J., Lebron, G., and Huygen, K.:** Heterologous expression of the *Mycobacterium tuberculosis* gene encoding antigen 85A in *Corynebacterium glutamicum*, Appl. Environ. Microbiol., **63**, 4392–4400 (1997).
37. **Ikeda, M., Mizuno, Y., Awane, S.-i., Hayashi, M., Mitsuhashi, S., and Tateno, S.:** Identification and application of a different glucose uptake system that functions as an alternative to the phosphotransferase system in *Corynebacterium glutamicum*, Appl. Microbiol. Biotechnol., **90**, 1443–1451 (2011).
38. **Majtan, T., Halgasova, N., Bukovska, G., and Timko, J.:** Transcriptional profiling of bacteriophage BFK20: coexpression interrogated by “guilt-by-association” algorithm, Virology, **359**, 55–65 (2007).
39. **Pátek, M. and Nešvera, J.:** Promoters and plasmid vectors of *Corynebacterium glutamicum*, pp. 51–88, in: Yukawa, H. and Inui, M. (Eds.), *Corynebacterium glutamicum*, biology and biotechnology. Springer-Verlag, Berlin, Heidelberg (2013).
40. **Maeda, T. and Wachi, M.:** 3′ Untranslated region-dependent degradation of the *aceA* mRNA, encoding the glyoxylate cycle enzyme isocitrate lyase, by RNase E/G in *Corynebacterium glutamicum*, Appl. Environ. Microbiol., **78**, 8753–8761 (2012).
41. **Palmer, T. and Berks, B. C.:** The twin-arginine translocation (Tat) protein export pathway, Nat. Rev. Microbiol., **10**, 483–496 (2012).
42. **Neidhardt, F. C., Ingraham, J. L., and Schaechter, M.:** Physiology of the bacterial cell: a molecular approach, pp. 1–29. Sinauer Associates, Inc., Sunderland (1990).